

# NMR Fingerprinting of Conventional and Genetically Modified Soybean Plants with AtAREB1 Transcription Factors

Isabel Duarte Coutinho,\* William Marcondes Facchinatto, Liliane Marcia Mertz-Henning, Américo José Carvalho Viana, Silvana Regina Rockenbach Marin, Silvia Helena Santagneli, Alexandre Lima Nepomuceno, and Luiz Alberto Colnago\*



Cite This: *ACS Omega* 2024, 9, 32651–32661



Read Online

ACCESS |



Metrics & More

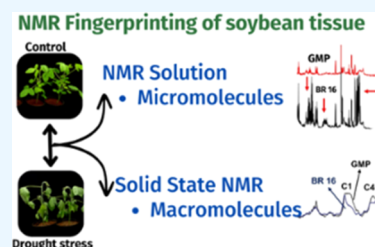


Article Recommendations



Supporting Information

**ABSTRACT:** Drought stress impacts soybean yields and physiological processes. However, the insertion of the activated form of the AtAREB1 gene in the soybean cultivar BR16, which is sensitive to water deficit, improved the drought response of the genetically modified plants. Thus, in this study, we used  $^1\text{H}$  NMR in solution and solid-state NMR to investigate the response of genetically modified soybean overexpressing AtAREB1 under water deficiency conditions. We achieved that drought-tolerant soybean yields high content of amino acids isoleucine, leucine, threonine, valine, proline, glutamate, aspartate, asparagine, tyrosine, and phenylalanine after 12 days of drought stress conditions, as compared to drought-sensitive soybean under the same conditions. Specific target compounds, including sugars, organic acids, and phenolic compounds, were identified as involved in controlling sensitive soybean during the vegetative stage. Solid-state NMR was used to study the impact of drought stress on starch and cellulose contents in different soybean genotypes. The findings provide insights into the metabolic adjustments of soybean overexpressing AREB transcription factors in adapting to dry climates. This study presents NMR techniques for investigating the metabolome of transgenic soybean plants in response to the water deficit. The approach allowed for the identification of physiological and morphological changes in drought-resistant and drought-tolerant soybean tissues. The findings indicate that drought stress significantly alters micro- and macromolecular metabolism in soybean plants. Differential responses were observed among roots and leaves as well as drought-tolerant and drought-sensitive cultivars, highlighting the complex interplay between overexpressed transcription factors and drought stress in soybean plants.



## 1. INTRODUCTION

Metabolomics refers to analytical profiling techniques used to understand how organisms respond to genetic and environmental changes. Nuclear magnetic resonance (NMR), chromatography, and mass spectrometry (MS) are the most used techniques for the metabolomic screening of plants. NMR is a powerful tool for structural assignment, providing structural information on a wide range of molecules at various levels.<sup>1–4</sup> NMR fingerprinting requires minimal sample preparation and can be performed on solid-state samples (SSNMR). It provides quantitative results, as the strength of a signal is directly proportional to the number of molecules responsible for the signal.<sup>5</sup> In solution,  $^1\text{H}$  NMR is the most used technique in the field, producing high-resolution spectra with good sensitivity due to its inherent high sensitivity and abundance in biological systems.

NMR-based plant metabolomics has the potential to provide new insights into the analysis of genetically modified plants, allowing for the detection of effects resulting from genetic engineering applications.<sup>6,7</sup> Several genetically modified crops have been studied using NMR-based analysis, including rice with genetically enhanced insect resistance,<sup>8</sup> maize with insect resistance<sup>9–11</sup> and herbicide tolerance,<sup>12</sup> wheat with enhanced nutrition,<sup>13</sup> and tomato with increased flavonol content,

improved texture, mouthfeel, and color.<sup>14</sup> NMR fingerprinting analysis can provide an overview of the physiological state of plants under stress conditions, and our group has been using a metabolic fingerprinting NMR approach to understand the response of soybean to flooding stress<sup>15</sup> and drought stress,<sup>16</sup> and *Campomanesia phaea*,<sup>17</sup> *Schiekia timida*,<sup>18</sup> and *Bahunia unguolata* to water stress.<sup>19</sup>

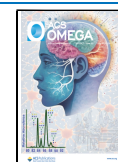
As mentioned above, due to the importance of the metabolomics approach in the chemical study of plants, we have employed  $^1\text{H}$  NMR in solution and SSNMR to investigate the response of genetically modified soybean under water deficiency conditions. Soybean is the most widely cultivated oil crop in the world and can be grown in diverse climatic regions. The cultivation has been highly concentrated in the United States, Brazil, Argentina, and China and used for oil and bran production for human and animal nutrition, biofuels production, cosmetics, pharmaceuticals, veterinary, and

Received: February 24, 2024

Revised: June 9, 2024

Accepted: June 12, 2024

Published: July 16, 2024



fertilizers.<sup>20,21</sup> In Brazil, the 2022/2023 soybean forecast predicts an expansion in planted area to 43.3 million ha and a record production of 153 million metric tons. While the season started well, the southern region may face crop issues without January rains.<sup>22</sup> Indeed, soybean production is strongly influenced by climate oscillations, such as drought, flooding, salt, and heat.<sup>23,24</sup> Among these environmental stresses, drought is the most widespread abiotic stress that severely impact soybean yield, growth, nutrient uptake, stomatal movement, and photosynthetic assimilate production.<sup>23,25,26</sup> There are potential leads for developing genetically drought-tolerant soybean, including genes involved in signal transduction pathways or transcription factors, such as DREBs that are involved in abscisic acid (ABA) signaling.<sup>27–31</sup> Marinho et al. demonstrated that soybean overexpressing the *Arabidopsis* ABA-Responsive Element Binding protein (AtAREB1) exhibited superior physiological responses to drought in a greenhouse. According to the authors, higher survival rates and better performance with regard to physiological, agronomical, and growth parameters of the transgenic AtAREB1 soybean line relative to the conventional cultivar may be related to the conservative use of water under well-watered conditions. Their results indicate that the constitutive overexpression of the transcription factor AtAREB1 leads to an improved capacity of the soybean to cope with water deficit conditions with no yield losses.<sup>32</sup> AREB is an important transcription factor triggered by abscisic acid.<sup>33–36</sup> ABA accumulates in plant cells and directs changes in gene expression and stomatal opening, resulting in decreased transpiration and water loss.<sup>37–39</sup> In studies performed by Fuganti-Pagliarini et al. in field conditions and Leite et al. in greenhouse, soybean transgenic lines expressing AtAREB1 also showed better performance compared to conventional cultivars in response to water deficiency.<sup>40,41</sup> Fuhrmann-Aoyagi et al. evaluated transgenic soybean line overexpressing the AtAREB1 under drought and flooding conditions. The results indicated that AtAREB1 activates cross-signaling responses under both stresses.<sup>42</sup> Soybean plants overexpressing AtAREB1 exhibited higher protein content, lower concentrations of hydrogen peroxide, and lower expression levels of genes related to fermentative metabolism and alanine biosynthesis.<sup>42</sup>

To the best of our knowledge, the effect of the transcription factor AtAREB1 on the soybean metabolome during water deficiency is unknown. Thus, in this study, we identified specific target compounds, such as soluble sugars, organic acids, amino acids, and phenolic compounds, that are involved in controlling plant tolerance during the vegetative stage under water deficiency. Additionally, we investigated the effect of drought stress on the metabolism of macromolecules using solid-state NMR. Our findings contribute to the understanding of the metabolic adjustments of soybean overexpressing AtAREB1 transcription factors in adapting to dry climates.

## 2. MATERIALS AND METHODS

**2.1. Chemicals.** Deuteriumoxide (99,9%), deuterated methanol (99,8%), 3-(trimethylsilyl propionic)-2,2,3,3-*d*<sub>4</sub> acid sodium (TSP-*d*<sub>4</sub>), ethylenediaminetetraacetic acid (>99,5%), potassium phosphate monobasic anhydrous (>99%), and potassium phosphate dibasic anhydrous (>98%) were purchased from Sigma-Aldrich (Darmstadt, Germany).

**2.2. Plant Material.** Seeds from soybean (*Glycine max* L. Merrill) tolerant genotypes, named 1Ea15 and 1Ea2939 (genetically modified events, GM) and from the cultivar

BR16 (conventional background, sensitive to water deficit), were germinated on paper moistened with a volume of water equivalent to 2.5 times the weight of dry paper for 96 h in a germination chamber at 25 ± 1 °C and relative humidity of 100%. Then, each seedling was transferred to a 1 L pot filled with a mixture of substrate and sand (1:1), with the substrate consisting of soil, sand, and organic compound (3:2:2). It was used with the randomized blocks experimental 3 × 2 factorial, relatively to three genotypes and four water conditions: 12 days of well-watered as control (C1), after water deficit (12 DWD), 14 days of well-watered as control (C2), and after water deficit (14 DWD). Three biological repetitions were used, each repetition consisting of a bulk of two plants. The seedlings were kept in a growth chamber with light at a programmed temperature of 28 ± 2 °C and received irrigation to maintain the substrate around 80% of the field capacity until the stress treatments were imposed. Stress by water deficit was imposed by suspension of irrigation when the plants reached the vegetative stage V3.<sup>43</sup> After the onset of stress, the plants were monitored daily in relation to stomatal conductance (gs) until they reached gs values of less than 200 mmol H<sub>2</sub>O/m<sup>2</sup> s<sup>-1</sup>,<sup>44</sup> totaling 8 days under water deficit. A set of plants representing the control group was kept under irrigation. At the end of the stress period, samples from the third fully expanded trifoliate leaf (apex-base direction) and from the roots were collected, packed separately in aluminum foil, immediately immersed in liquid nitrogen, stored at -80 °C, lyophilized, and milled for the metabolic analyses.

### 2.3. Sample Preparation for Metabolomics Analysis.

The extracts were obtained from 50 mg of tissue (root and leaf) milled leaves and 1.00 mL of CD<sub>3</sub>OD/D<sub>2</sub>O (80:20 v/v). The contents of the tube were vortexed for 30 s and sonicated for 10 min at 50 °C. Then, the samples were cooled and centrifuged for 5 min at 4 °C and an aliquot of 700 μL of supernatant was stored for 30 min. Then, 20 μL of 2.40 mM phosphate buffer was added to each extract.<sup>45</sup> The samples were stored at 4 °C for 18 h, and 10 μL of sodium salt of trimethylsilyl propionic acid (TSP-*d*<sub>4</sub>) at 0,02 mol/L was added in 600 μL from each extract of leaves and transferred to a 5 mm NMR tube. For roots samples, besides TSP-*d*<sub>4</sub>, 10 μL of EDTA at 40 mmol/L was added to 600 μL of samples and transferred to an NMR tube.

**2.4. Solution <sup>1</sup>H NMR Spectroscopy.** <sup>1</sup>H NMR spectroscopy was performed at 14.1 T (600 MHz for <sup>1</sup>H observation) at 25 °C using an Advance 600 Bruker NMR spectrometer (Karlsruhe, Germany) equipped with a 5 mm BBO probe. The proton spectra were acquired using nuclear overhauser effect spectroscopy (NOESY) 1D with a 4.00 s presaturation delay and acquisition time of 1.69 s (64k points), accumulation of 256 transients, and spectral width of 15 ppm. All of the FIDs were automatically Fourier transformed after the application of an exponential window function with a line broadening of 0.3 Hz. Phasing and baseline corrections were carried out within the TopSpin software. <sup>1</sup>H NMR chemical shifts were referenced to TSP-*d*<sub>4</sub> at δ 0.00. 2D *J*-resolved and heteronuclear single quantum correlation (HSQC) experiments were acquired using a standard pulse sequence available to support metabolite identifications. The 1D spectra of soybean leaves and roots were assigned according to previous work of Coutinho et al.<sup>15</sup>

**2.5. Solid-State <sup>1</sup>H and <sup>13</sup>C NMR Spectroscopy.** The experiments were performed using an Avance III 400 WB HD SSNMR spectrometer (Karlsruhe, Germany) operating at 9.4

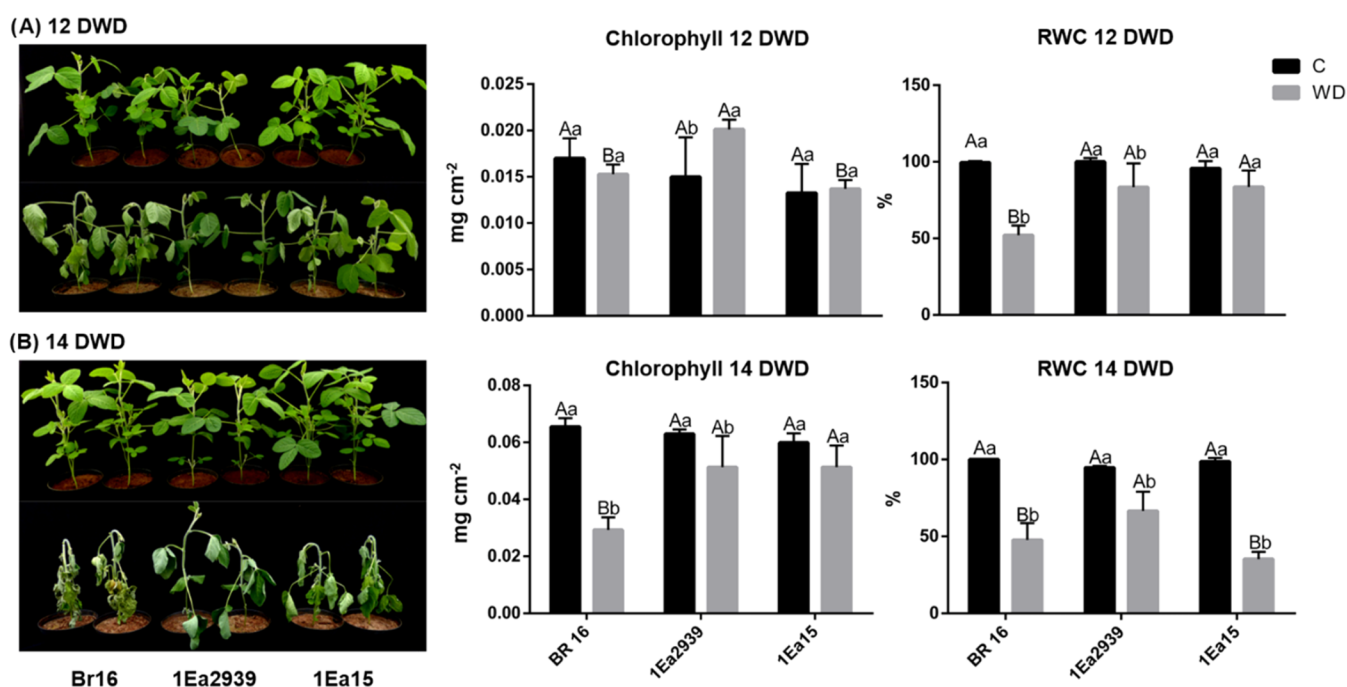


**Figure 1.** Visual phenotype of soybean plants of control (above) and BR16 (sensitive) and 1Ea15 and 1Ea2939 (tolerant) genetically modified plant (below) after 12 DWD (A) and 14 DWD (B). Content of chlorophyll per leaf area (mg/cm<sup>2</sup>) and relative water content, RWC (%), measured in soybean after 12 DWD (A) and 14 DWD (B). The means ( $n = 6$ ) and standard deviation, represented by columns and bars, respectively, followed by similar capital letters (between water conditions) and lowercase letters (between genotypes) do not differ by Tukey's test ( $p \leq 0.05$ ).

T, using a commercial double resonance of 4 mm. Typical spinning speeds were 12 kHz. The samples were packed in zirconia rotors of 4 mm. <sup>13</sup>C{<sup>1</sup>H} MultiCP-MAS spectra (cross polarization and magic angle spinning) were acquired using a spectral width of 416 kHz, an acquisition time of 25 ms, <sup>1</sup>H pulse length of 4.8  $\mu$ s, a contact time of 3.0 ms (a linear ramp on the <sup>1</sup>H contact pulse 30% slope), and a recycled delay of 2 s.<sup>46,47</sup> All spectra were acquired under TPPM-15 proton decoupling during the data acquisition by applying decoupling pulses of 5.8  $\mu$ s. <sup>1</sup>H-MAS spectra have been acquired using a pulse sequence that incorporates a T2 filter (spin echo) and an exchange block of  $t = 1$  ms.

**2.6. Multivariate Analysis.** The <sup>1</sup>H NMR data were arranged in an  $X_{IJ}$  matrix, where  $I$  corresponded to the samples, 36, and  $J$  corresponded to the columns of 64k variables. The NMR data were aligned by using the *icoshift* algorithm. Then, the region corresponding to residual signal of water and TSP was excluded. The data preprocessing and partial least square–discriminant analysis (PLS-DA) from <sup>1</sup>H NMR were performed using MATLAB R2016b and PLS-Toolbox from normalized and mean-centering data. CHE-NOMX software (NMR suite 9.0 evaluate version) was used to calculate the levels of 31 metabolites as measured by <sup>1</sup>H NMR. The exported data were analyzed using the Metaboanalyst web server ([www.metaboanalyst.ca](http://www.metaboanalyst.ca))<sup>48</sup> with fold change statistical analysis normalized by the sum. For fold change statistical analysis, an average of the relative metabolite concentrations among two harvest periods of cultivars (BR16, 1Ea2939, and 1Ea15) was used to propose a metabolic pathway related to impact of the water deficit stress on the genotypes.

**2.7. Univariate Statistical Analysis.** Data from physiological parameters and metabolomic analysis showed a normal distribution and were submitted to the analysis of variance

(ANOVA). The comparison of means was performed by the Tukey test ( $p \leq 0.05$ ), using SISVAR software.<sup>49</sup> The simple effects of genotype (G) or water condition (WC) are shown in tables, whereas interaction effects ( $G \times WC$ ) are shown in graphics.

### 3. RESULTS AND DISCUSSION

**3.1. Chlorophyll and Relative Water Content.** Chlorophyll and relative water content were evaluated to prove that plants were under water stress, and treatments were performed properly before NMR fingerprinting analysis of the samples. After 12 DWD and 14 DWD, the photosynthetic pigment (chlorophyll content) index was higher in Genetically Modified Plants (GMP; 1Ea15, and 1Ea2939) compared to non-GMP (BR16) (Figure 1C,D), suggesting a possible adaptive response of the GM genotypes.

Another important parameter analyzed related to water deficit was the leaf relative water content (RWC), which showed a significant reduction of 50, 15, and 15% in BR16, 1Ea2939, and 1Ea15 genotypes, respectively, after 12 DWD compared to control conditions and 50, 25, and 60% after 14 DWD compared to control conditions (Figure 1). Decreased RWC is an early response to water deficit and represents variations in osmotic adjustment, as previously observed in the drought-sensitive BR16 genotype.<sup>50</sup> When comparing the RWC of the sensitive genotype to GMP, the RWC of GMP showed a smaller decrease, mainly after 12 DWD. The visual phenotype of the drought-sensitive genotype compared to the tolerant one was compatible with typical symptoms of water deficiency (Figure 1A,B).

**3.2. Water Limitation Effects on Metabolite Profiles of Soybean Leaves and Roots.** The plants developed various adaptive strategies to cope with drought stress,

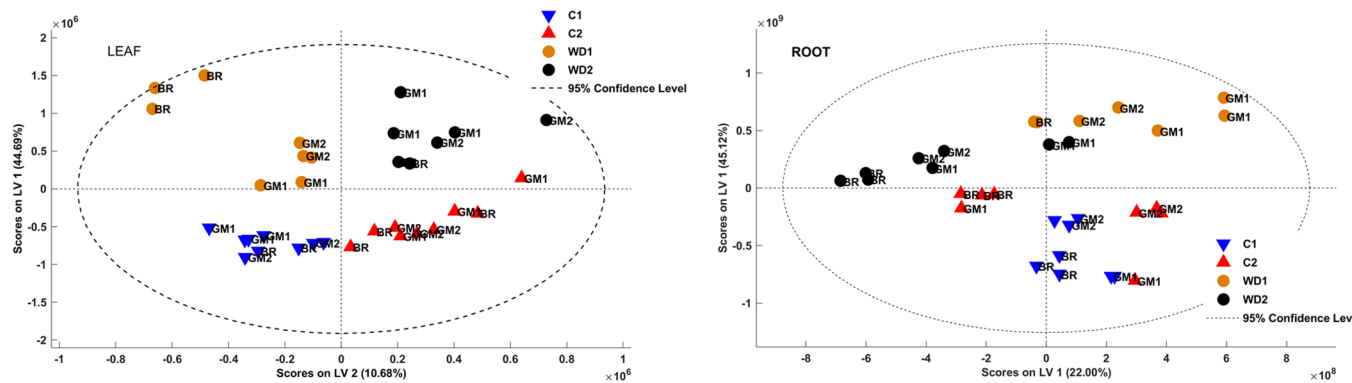


**Figure 2.** PLS-DA model from  $^1\text{H}$  NMR spectra extracts from soybean leaves and roots of sensitive genotype BR16 (BR) and tolerant genetically modified plants 1Ea2939 (GM1) and 1Ea15 (GM2). C1 and C2 correspond to well-watered treatment during 12 days (C1) and 14 days (C2); WD1 and WD2 correspond to water deficit treatment after 12 days of water deficit (WD1) and 14 days of water deficit (WD2).

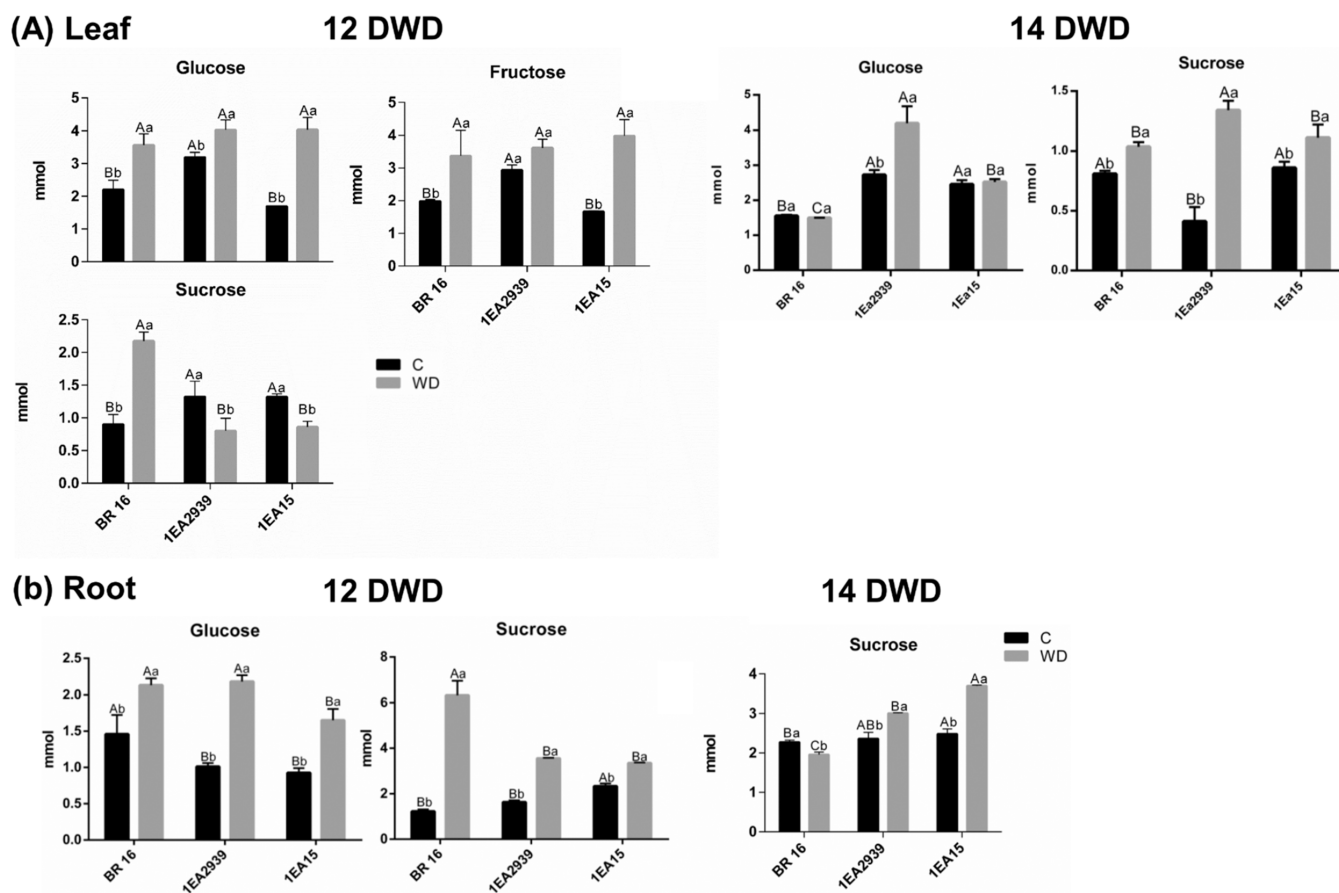


**Figure 3.** Carbohydrate content in leaves (a) and roots (b) of genetically modified genotypes (1Ea2939 and 1Ea15) and conventional cultivar (BR16) under control and water deficit (WD) conditions. The means ( $n = 6$ ) and standard deviation are represented by columns and bars, respectively. In each treatment, capital letters compare the water conditions, and lowercase letters compare the genotypes. Means followed by equal letters do not differ by Tukey's test ( $p \leq 0.05$ ).

including modifications in physiological and molecular mechanisms. To provide a comparative interpretation and visualization of metabolic changes among soybean genotypes, the supervised partial least-squares discriminant analysis (PLS-DA) method was applied to the  $^1\text{H}$  nuclear magnetic resonance (NMR) data. The study included soybean leaf and root samples from three genotypes, including one drought-sensitive conventional cultivar (BR16) and two drought-tolerant GMP (1Ea15 and 1Ea2939) soybean genotypes. Metabolic differences between the sensitive and GMP were

visualized using two latent variables, which revealed that the metabolic profiling of the BR16 genotype was significantly altered in response to drought stress compared with the GMP (Figure 2).

Based on Figure 2, left, the PLS-DA score plot of two latent variables clearly showed discrimination between soybean genotypes under water deficit and control conditions. The differences between BR16 and GMP genetically modified (GM) leaves were more distinct in response to water deficit, with samples located in positive LV1 showing high correlation

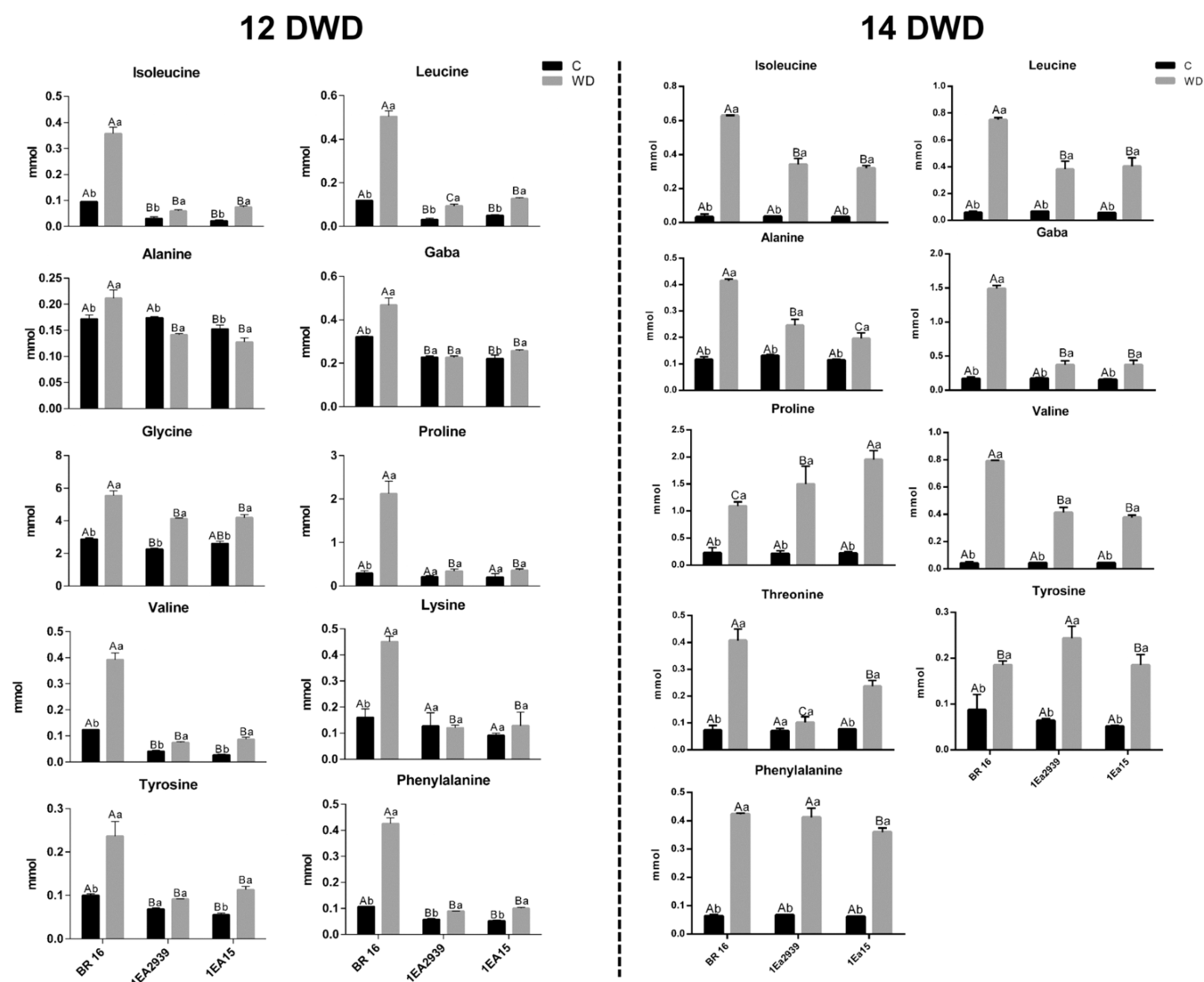


**Figure 4.** Amino acids content in leaves of 1Ea2939, 1Ea15 and BR16 under control and water deficit (WD) conditions. The means ( $n = 6$ ) and standard deviation are represented by columns and bars, respectively. In each treatment, capital letters compare the water conditions and lowercase letters compare the genotypes. Means followed by equal letters do not differ by Tukey's test ( $p \leq 0.05$ ).

with signals corresponding to amino acids and sugars (as shown in the loading plot of LV1). Interestingly, LV2 led to clustering based on days of harvest, with genotypes harvested at 12 DWD located at negative LV1; while samples submitted to 14 DWD were clustered at positive LV1. The loadings plot in Figure S1 revealed the contribution of different variables to the discriminating ability of each PLS-DA model. Both latent variables one and two from PC1 and PC2 indicated clear metabolic variation between well-watered and drought conditions. According to the loading plot of LV2, the main difference between days of stress was due to the oscillation of patterns of signals corresponding to citric acid, sugars, and phenolic compounds.

Similarly, the PLS-DA model from  $^1\text{H}$  NMR spectra of soybean root polar extracts (Figure 2, right) showed a similar pattern to that of the soybean leaves model in terms of stress conditions. The discrimination was mainly due to an increase in sucrose levels and a decrease in citric acid and isoflavone levels in response to drought stress (as shown in Figure S1). Furthermore, the oscillation in isoflavone levels appeared to be an important target in the root's response to water deficit. The

discrimination between GM soybean and BR16 cultivars was clear in soybean roots under 14 DWD, with samples located at positive and negative LV2.

**3.3. Accumulation of Putative Osmolytes.** The direct analysis by NMR offers the advantage of detecting a wide range of metabolites in a quantitative and unbiased manner. In this study, we identified a total of 31 metabolites in soybean leaves and root extracts, including various carbohydrate metabolites (such as sucrose, glucose, pinitol, and *myo*-inositol), amino acids (such as leucine, isoleucine, valine, proline, glycine, phenylalanine, tyrosine, alanine, threonine, asparagine, lysine, and GABA), organic acids (such as citrate, malate, lactate, acetate, succinate, glutamate, formate, and fumarate), phenolic compounds (such as *cis*-coumaroylquinic acid, *trans*-coumaroylquinic acid, and three kaempferol derivatives), as well as choline and trigonelline. The relative content of amino acids, sugars, organic acids, and phenolic compounds was monitored to evaluate the fluctuations in the metabolome of soybean leaves and roots under different stress periods (12 and 14 DWD), and the contents were compared with those of the respective control. We observed in both leaves and roots that

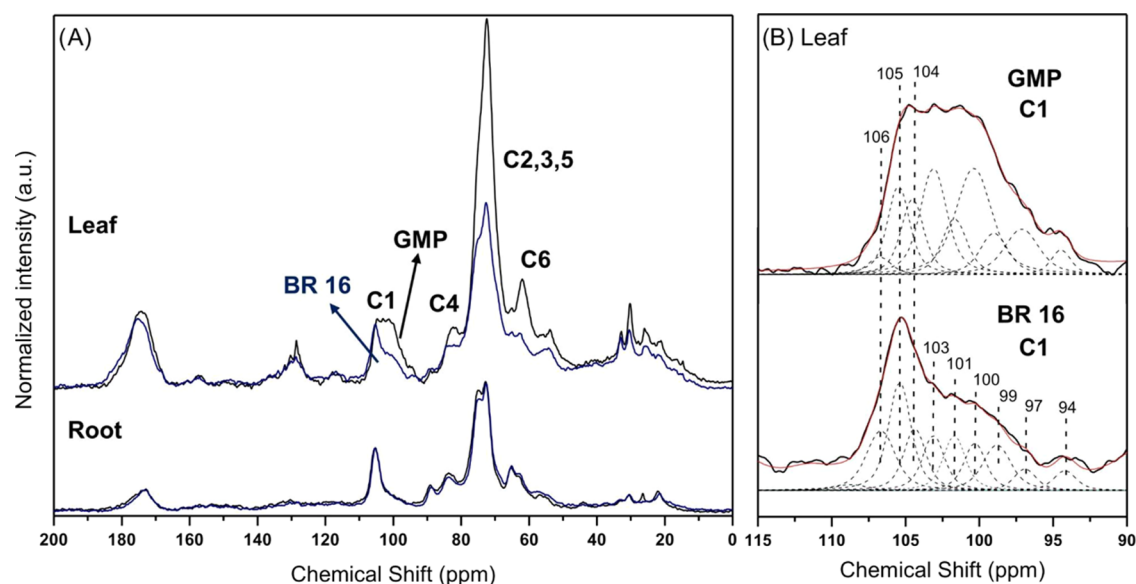


**Figure 5.** SSNMR spectra of lyophilized soybean leaves and roots from GMP and BR16 samples normalized by the C1 carbon signal (A). Deconvolution assignment from cellulose and starch contributions to C1 (B).

the drought stress significantly altered the levels of most of the metabolites, including carbohydrate (Figure 3), amino acid content in leaves (Figure 4), and other metabolites (Figures S1–S3). The simple effects of the water status and genotype are shown in Tables S1 and S2, respectively. Taken together, these results indicated that water limitation led to the accumulation of several metabolites during the stress period.

The results showed significant interactions between stress conditions and genotypes for several metabolites, particularly in the sensitive genotype BR16, as shown in Figures 3 and 4. Genotype effects were also observed in both the leaves and roots. The sensitive genotype BR16 exhibited higher accumulation of several compounds compared to the GMP (Table S2). Specifically, a remarkable accumulation of amino acids was observed in both leaves and roots of BR16 cultivar after 12 DWD (Figures 4 and S2). Additionally, differences were noted in the pattern of glucose and fructose accumulation, with glucose levels being higher in the 1Ea2939 genotype compared to those in BR16 and 1Ea15 after 14 DWD (Figure 3). Notably, sucrose levels decreased in GMP after 12 DWD, while the opposite trend was observed in the sensitive cultivar (Figure 3). However, after 14 DWD, sucrose accumulation increased in all genotypes.

In the leaves, the effect of stress on genetically modified soybean was lower compared to that of the sensitive cultivar, with significant variations in levels of amino acids, glucose, and sucrose observed mainly after 14 DWD (Figures 3 and 4). Organic acids also showed differences among genotypes, with slight metabolic fluctuations in acetate and fumarate levels and notable accumulations of citrate, glutamate, succinate, and lactate (Figures S3 and S4). Malic and succinic acid increased in BR16 and 1Ea15 genotypes but decreased in the 1Ea2939 genotype during water limitation. Citric acid content was generally lower in response to water deficiency, while lactate levels increased in all genotypes. Organic sugars such as pinitol and *myo*-inositol increased in all genotypes under drought conditions, along with choline, trigonelline, and 2-hydroxyisobutyrate. These findings highlight the significant impact of water deficit on the metabolite profiles of soybean leaves and

roots and the differential responses of genotypes, including genetically modified plants, to water deficit conditions.

In the roots, the levels of amino acids and sugars increased after 12 and 14 DWD, except for alanine in 1Ea2939 after 12 DWD, as previously observed in the leaves' metabolome. The amino acids isoleucine, leucine, proline, valine, and asparagine were detected only in plants subjected to drought stress, and the levels of glucose and sucrose were 1.4 and 5.2 times higher in plants subjected to water deficit conditions compared to control plants. Regarding organic acids, quantitative changes were observed in the tricarboxylic acid cycle in response to drought stress. The levels of citric and succinic acid were significantly reduced in the roots after 12 DWD. However, a decrease in citrate levels was observed in both roots and leaves after 14 DWD. The abundance of *myo*-inositol was altered by drought stress, with opposite patterns observed in leaves and roots (Figures S3 and S4). Decreased levels of metabolites were observed in roots, while increased levels of metabolites were observed in leaves. Choline levels increased in both leaves and roots, but in roots it tended to decrease in the 1Ea15 genotype (Figures S3 and S4).

The relative concentrations of isoflavones, hydroxycinnamic acids, and kaempferol derivatives were determined based on specific areas of the corresponding signals in the  $^1\text{H}$  spectra. The concentration of daidzin decreased in the roots in response to water deficiency in all genotypes after 12 DWD (Figure S5). Interestingly, the levels of daidzein decreased in the 1Ea2939 genotype, but increased in the 1Ea15 genotype (Figure S5). Hydroxycinnamic acid and kaempferol glycosides were detected only in soybean leaves. The changes in the profile of hydroxycinnamic acids were quite similar among genotypes, but the adjustments in the kaempferol levels were different. Drought-sensitive genotypes showed higher concentrations of kaempferol glycosides in control conditions compared with GMP, but these levels significantly decreased in response to water limitation. On the other hand, in GMP, the abundance of kaempferol increased in response to water deficit (Figure S6).

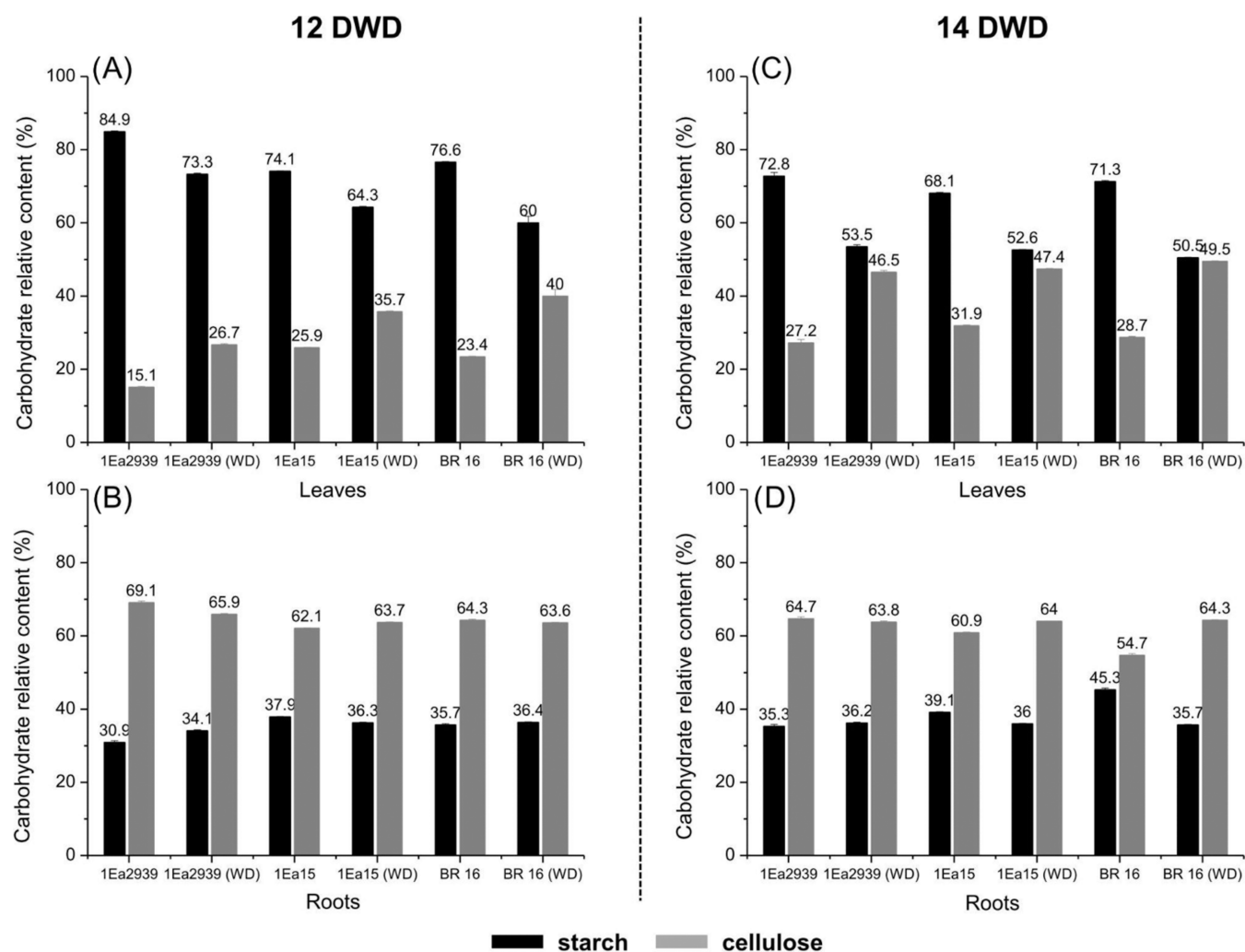


**Figure 6.** Quantification of cellulose and starch using the C1 carbon signal from  $^{13}\text{C}$  SSNMR spectra of leaves and roots from GMP and Br16 samples under 12 (A, B) and 14 (C, D) DWD conditions.

Compared to BR16 plants, GMP performed better in the field, attributed to its ability to prevent drought through reduced stomatal conductance and leaf transpiration under normal conditions.<sup>40</sup> Marinho et al. suggested that constitutive overexpression of the transcription factor AtAREB1 enhances the drought tolerance of the 1Ea2939 genotype without incurring yield losses.<sup>32</sup> Our findings indicate that important molecules involved in maintaining cell turgor are synthesized at a later stage in tolerant genotypes compared to BR16 genotypes. Notably, a rapid increase in putative osmolyte content was observed in tolerant genotypes after 14 DWD. Alanine content also increased in response to water deficiency, but the magnitude of the increase varied among genotypes based on their sensitivity.

Distinct patterns in sugar accumulation were observed among genotypes under both control and drought conditions. In leaves, line 1Ea2939 exhibited a higher sugar content under control conditions, with increased levels of glucose and fructose observed in response to water deficiency. In the roots, all genotypes showed remarkable accumulation of carbohydrates after 12 DWD. Sugars can also act as signaling molecules, interacting with the ABA-dependent signaling pathway to activate components in the stress response cascade. Rapid biosynthesis of ABA was found to be correlated with

stress-induced changes in starch metabolism.<sup>51</sup> Thalmann and Santelia showed that the effect of ABA on starch metabolism is partly mediated by ABA-responsive element binding factors (AREB), and this mechanism seems to be conserved among eudicots.<sup>52</sup>

**3.4. Polysaccharide and Lipid Profiles by SSNMR Spectroscopy.** SSNMR experiments were conducted using the quantitative MultiCP pulse sequence to identify the relationship between the spectral profiles of lyophilized soybean leaves and roots in terms of cellulose and starch variability. Figure 5 provides an overview of the  $^{13}\text{C}$  signal shape dependence from these polysaccharides recorded at different ratios, the main variability assigned to real samples spectra, while the overall tendency after DWD conditions for each genotype is shown in Figure 6.

As the leaves and roots are predominantly composed and structured by lignocellulose and starch at varying ratios, prior signal assignments to the  $^{13}\text{C}$  NMR spectra of pure and standard compounds seemed advantageous, considering that the signals of the glucopyranose ring, which are present in both cellulose and starch, are commonly overlapped. To achieve the correct assignment of cellulose and starch contributions in the compositions of leaves and roots, a specific weight of pure compounds was mixed in predetermined proportions. The

respective  $^{13}\text{C}$  NMR spectra of cellulose, starch, and their mixtures are shown in Figure S7. It is worth noting that anomeric carbon C1 was useful for quantifying the percentage of the compounds, and the deconvoluted values closely matched the weight proportions. Although the other  $^{13}\text{C}$  signals also vary with respect to the compound content, the relative distinction is biased, and the quantification through these signals is at least doubtful due to complete signal overlap across a broad range, which is not the case for the C1 signal. An additional morphological dependence, which is evident in all cellulose and starch signals, also plays a role in the correct assignment and contribution in a given mixture of the two polysaccharides. It should be considered that the crystallinity indexes inside the leaves and roots is unknown. While the C1 carbon signal from cellulose shows no significant variation, the one from starch is severely affected by morphological variations, as can be seen in Figure S8. Fortunately, despite this clear dependence, the deconvolution procedure was able to overcome this issue as the C1 signal overlap between cellulose and starch is negligible. Therefore, C1 was employed to accurately quantify the levels of cellulose and starch consumption in the leaves and roots of the GMP and Br16 samples.

Figure 5 shows  $^{13}\text{C}$  NMR spectra normalized to  $\delta$  102–105 ppm signal intensity of the lyophilized soybean leaves and roots under water deficit and control. The spectral regions were attributed according to literature and starch and cellulose standards.<sup>53–59</sup> Six different chemical shift regions were clearly observed in both spectra (leaf and root). In leaves spectra, signals  $\delta$  101–105 ppm were assigned to C-1 of the starch glycosidic unit, the  $\delta$  72 ppm signal was assigned to carbons 2, 3, and 5, signal  $\delta$  83 ppm for C-4 and  $\delta$  62 ppm corresponding to C-6. The signals at  $\delta$  120–140 ppm were assigned to the aromatic carbons of lignin and proteins. The region between  $\delta$  165 and 180 ppm was attributed to the acyl functional group (C=O) of aliphatic carboxylic acids, esters, and amide groups of proteins ( $\delta$  173 ppm). The main qualitative difference between the  $^{13}\text{C}$  spectra of leaves and roots of lyophilized soybean is related to the pattern of C1, C4, and C6 atom signals. Signals from  $\delta$  105 to  $\delta$  60 ppm were attributed to starch in leaves, while the same region was attributed to cellulose in soybean roots. According to the deconvolution of the C1 carbon signal, soybean leaves clearly show a major content of starch, whereas cellulose plays this whole in roots.

The deconvolution procedure was applied to all samples, and a similar trend was observed regardless of the genotype, as mentioned earlier (Figure S7). However, the gap between cellulose and starch content appeared to decrease from 12 to 14 DWD in leaves, rather than in the roots. This overall trend supports the previous finding in Figure 3, indicating an increase in the levels of sugar molecules, likely resulting from the hydrolysis of cellulose and starch.

$^1\text{H}$  NMR experiments were conducted using the  $^1\text{H}$  ECHO-MAS pulse sequence to obtain spectral profiles of compounds with lower mobility, such as lipids (Figure S9). The signals corresponding to methyl and methylene groups, as well as signals at  $\delta$  5.15 and 5.37 ppm, were assigned to  $^1\text{H}$  in unsaturated linkages (Table S3). No signal was observed at  $\delta$  4.2 ppm, indicating the absence of glycerol units, triacylglycerols, and phospholipids,<sup>60</sup> which suggests the presence of free fatty acids. Additionally, the intense signal at  $\delta$  0.97 ppm is likely attributed to methyl groups of the terpene unit. The main difference observed in the  $^1\text{H}$  NMR spectra of lyophilized

soybean leaves between conventional genotypes and PGM under stress and control conditions is the lower intensity of spectral lines relative to the BR16 conventional cultivar in response to a water deficit.

The increase in sugar content is largely attributed to starch hydrolysis, which requires enzymes with hydrolytic activity.<sup>61</sup> Starch is a glucose polymer synthesized in plant plastids and algae consisting of two types of polymers: amylose, which is linear and has small chains linked by  $\alpha$ -(1–4) bonds, and amylopectin, which is branched and has large  $\alpha$ -(1–6) chains. Amylopectin constitutes 70–90% of the starch granules in plants. In leaves, starch is degraded within the plastids where it is synthesized.<sup>62</sup> These polymers adopt secondary and tertiary complex structures, organizing insoluble and crystalline granules to store energy in a dense and osmotically inert form.<sup>63</sup>

Our findings have demonstrated that the introduction of AtAREB1 transcription factors in soybean plants can effectively mitigate the symptoms caused by drought stress and maintain sucrose flow even under drought conditions. Additionally, the content of starch in leaves decreased under stress conditions, indicating that drought stress triggers starch degradation into sucrose.<sup>62,64</sup> Specifically, they observed a 15% reduction in starch content in leaves of genetically modified soybeans, whereas starch content increased in seeds under both control and stress conditions. According to Boyer, in the absence of photosynthetic products, starch is eventually depleted, and glucose levels decrease in the ovary and supporting structures during drought stress.<sup>65</sup> Furthermore, even when the delivery of photosynthetic products is limited at low water potentials during drought, enzymes that convert sucrose to glucose lose activity, and starch is consumed, as stated by the authors.

It is worth noting that plants contain two types of starch that are structurally indistinguishable: secondary starch and transitional starch. These types of starch are mainly differentiated based on the storage organs and rates of synthesis and storage.<sup>66</sup> During the day, starch is stored in the chloroplasts of mesophyll cells and remobilized at night to provide carbon and energy for maintenance and growth. These short-term reserves, known as transient starch, are also found in the chloroplasts of guard cells and around the pores of stomata.<sup>63</sup> Transient starch is degraded in the presence of light, generating organic acids and sugars that increase guard cell turgor and promote stomatal opening.<sup>63,67</sup>

Guard cells play a critical role in plant survival and productivity, as they regulate the opening and closing of stomata in response to internal and external factors, thus optimizing  $\text{CO}_2$  assimilation for photosynthesis while minimizing excessive water loss through transpiration. Studies have shown that starch metabolism in guard cells is responsible for rapid stomatal opening in the presence of light and in response to water deficit.<sup>63,68,69</sup>

The sensitive genotype exhibited a distinct pattern of  $^1\text{H}$  ECHO spectra corresponding to lipids, with a lower signal intensity compared to tolerant samples. Lipids are essential constituents of plant cells, comprising approximately 5 to 10% of the dry mass, with the majority found in membranes. Fatty acids in cells are typically esterified or modified, with almost all fatty acids in membranes being esterified to glycerol, forming glycerolipids.<sup>70</sup> Free fatty acids, which are not esterified with glycerol, are utilized in the biosynthesis of malonyl-CoA.

Membranes are the primary targets of degradation induced by water deficit, and studies have shown that a decrease in lipid



content in membranes is correlated with inhibition of lipid biosynthesis and stimulation of lipolytic and peroxidative activities in response to water deficit. Research has also demonstrated that genotypes of *Arabidopsis thaliana* (Columbia Ecotipo) with resistance to water deficit exhibit high tolerance due to the stability of the lipid content in leaves. This suggests that changes in membrane lipid composition under severe water stress may lead to conformational changes in membrane proteins and alterations in cellular ultrastructure.

In this study, we present novel solid and liquid NMR techniques for investigating the metabolome of transgenic soybean plants in response to water deficit. Our methods involve the identification and quantification of micro- and macromolecules. The  $^1\text{H}$  NMR analyses enabled the identification of a diverse array of primary and secondary metabolites, including sugars and amino acids, in leaves and roots under drought stress conditions. Additionally, we utilized SSNMR to determine the impact of drought stress on starch and cellulose contents in soybean genotypes. Unlike conventional methods that require meticulous sample preparation, our SSNMR analyses were conducted directly on lyophilized tissue. Consequently, our approach allowed for identification of physiological and morphological changes in drought-resistant and drought-tolerant soybean tissues following the water stress period. Indeed, drought stress significantly alters the micro- and macromolecular metabolism of soybean plants, with many affected compounds implicated in carbon and nitrogen metabolism. Notably, differential responses were observed between roots and leaves as well as among drought-tolerant and drought-sensitive cultivars.

## ■ ASSOCIATED CONTENT

### SI Supporting Information

The Supporting Information is available free of charge at <https://pubs.acs.org/doi/10.1021/acsomega.4c01796>.

Details of PCA loadings from PLS-DA model from  $^1\text{H}$  NMR spectra and content of metabolites have been showed in Figures S1–S7. The  $^{13}\text{C}$  SSNMR spectra shape profile and  $^{13}\text{C}$  NMR spectra from cellulose, starch, and samples have been showed in Figures S8 and S9, respectively. The water condition effect is described in Tables S1–S3. (PDF)

## ■ AUTHOR INFORMATION

### Corresponding Authors

Isabel Duarte Coutinho – *Embrapa Instrumentation, Brazilian Agricultural Research Corporation, 13560-970 São Carlos, São Paulo, Brazil*; [orcid.org/0000-0002-7795-6129](https://orcid.org/0000-0002-7795-6129); Phone: +5516997699125; Email: [isadcoutinho@hotmail.com](mailto:isadcoutinho@hotmail.com)

Luiz Alberto Colnago – *Embrapa Instrumentation, Brazilian Agricultural Research Corporation, 13560-970 São Carlos, São Paulo, Brazil*; Email: [luiz.colnago@embrapa.br](mailto:luiz.colnago@embrapa.br)

### Authors

William Marcondes Facchinatto – *Embrapa Instrumentation, Brazilian Agricultural Research Corporation, 13560-970 São Carlos, São Paulo, Brazil*  
Liliane Marcia Mertz-Henning – *Embrapa Soybean, Brazilian Agricultural Research Corporation, 86085-981 Londrina, Paraná, Brazil*

Américo José Carvalho Viana – *Embrapa Soybean, Brazilian Agricultural Research Corporation, 86085-981 Londrina, Paraná, Brazil*; [orcid.org/0000-0001-9509-0093](https://orcid.org/0000-0001-9509-0093)

Silvana Regina Rockenbach Marin – *Embrapa Soybean, Brazilian Agricultural Research Corporation, 86085-981 Londrina, Paraná, Brazil*

Silvia Helena Santagneli – *Institute of Chemistry, São Paulo State University (UNESP), CEP 14800-060 Araraquara, São Paulo, Brazil*

Alexandre Lima Nepomuceno – *Embrapa Soybean, Brazilian Agricultural Research Corporation, 86085-981 Londrina, Paraná, Brazil*

Complete contact information is available at:

<https://pubs.acs.org/10.1021/acsomega.4c01796>

## Author Contributions

I.D.C.: Data curation, conceptualization, writing—original draft preparation, writing—review and editing, methodology, formal analysis and investigation, project administration. W.M.F.: Data curation, writing—original draft preparation, writing—review and editing, methodology, formal analysis, and investigation. L.M.M.-H.: Resources, methodology. A.J.C.V.: Software. S.R.R.M.: Methodology. S.H.S.: Methodology. A.L.N.: Resources. L.A.C.: Conceptualization, funding acquisition, writing—review and editing, supervision. I.D.C. and W.M.F. conceived and designed research, analyzed data and wrote the manuscript. I.D.C., W.M.F., A.J.C.V., and S.H.S. conducted experiments. L.M.M.-H., S.R.R.M., and A.L.N. provided the resources and supplies. L.A.C. provided the funding.

## Funding

This work was supported by grants from the São Paulo Research Foundation (FAPESP Grant Numbers 2016/20970-2, 2019/13656-8, 2021/12694-3), and National Council for Scientific and Technological Development (CNPq Grant Number 307635/2021-0). This study was financed in part by National Council for the Improvement of Higher Education – Brazil (CAPES) – Finance Code 001.

## Notes

The authors declare no competing financial interest.

## ■ ACKNOWLEDGMENTS

The authors thank the assistance provided by the Embrapa Instrumentação and Institute of Chemistry (UNESP) for the NMR measurements and Embrapa Soja for treatment of soybean under drought conditions.

## ■ REFERENCES

- (1) De Jonge, N. F.; Mildau, K.; Meijer, D.; Louwen, J. J. R.; Bueschl, C.; Huber, F.; van der Hooft, J. J. J. Good practices and recommendations for using and benchmarking computational metabolomics metabolite annotation tools. *Metabolomics* **2022**, *18* (12), 103.
- (2) Guillén, M. D.; Ruiz, A. High resolution  $^1\text{H}$  nuclear magnetic resonance in the study of edible oils and fats. *Trends Food Sci. Technol.* **2001**, *12* (9), 328–338.
- (3) Judge, M. T.; Ebbels, T. M. D. Problems, principles and progress in computational annotation of NMR metabolomics data. *Metabolomics* **2022**, *18* (12), 102.
- (4) Otify, A. M.; El-Sayed, A. M.; Michel, C. G.; Farag, M. A. Metabolites profiling of date palm (*Phoenix dactylifera* L.) commercial by-products (pits and pollen) in relation to its antioxidant

effect: a multiplex approach of MS and NMR metabolomics. *Metabolomics* **2019**, *15* (9), 119.

(5) Ciampa, A.; Danesi, F.; Picone, G. NMR-Based Metabolomics for a More Holistic and Sustainable Research in Food Quality Assessment: A Narrative Review. *Appl. Sci.* **2023**, *13* (1), No. 372, DOI: 10.3390/app13010372.

(6) Bedair, M.; Glenn, K. Evaluation of the use of untargeted metabolomics in the safety assessment of genetically modified crops. *Metabolomics* **2020**, *16* (10), 111.

(7) Simó, C.; Ibáñez, C.; Valdés, A.; Cifuentes, A.; García-Cañas, V. Metabolomics of genetically modified crops. *Int. J. Mol. Sci.* **2014**, *15* (10), 18941–18966.

(8) Keymanesh, K.; Darvishi, M. H.; Sardari, S. Metabolome Comparison of Transgenic and Non-transgenic Rice by Statistical Analysis of FTIR and NMR Spectra. *Rice Sci.* **2009**, *16* (2), 119–123.

(9) Manetti, C.; Bianchetti, C.; Bizzarri, M.; Casciani, L.; Castro, C.; D'Ascenzo, G.; et al. NMR-based metabolomic study of transgenic maize. *Phytochemistry* **2004**, *65* (24), 3187–3198.

(10) Manetti, C.; Bianchetti, C.; Casciani, L.; Castro, C.; Di Cocco, M. E.; Miccheli, A.; et al. A metabolomic study of transgenic maize (*Zea mays*) seeds revealed variations in osmolytes and branched amino acids. *J. Exp. Bot.* **2006**, *57* (11), 2613–2625.

(11) Piccioni, F.; Capitani, D.; Zolla, L.; Mannina, L. NMR metabolic profiling of transgenic maize with the Cry1Ab gene. *J. Agric. Food Chem.* **2009**, *57* (14), 6041–6049.

(12) Barros, E.; Lezar, S.; Anttonen, M. J.; van Dijk, J. P.; Röhlig, R. M.; Kok, E. J.; Engel, K.-H. Comparison of two GM maize varieties with a near-isogenic non-GM variety using transcriptomics, proteomics and metabolomics. *Plant Biotechnol. J.* **2010**, *8* (4), 436–451.

(13) Baker, J. M.; Hawkins, N. D.; Ward, J. L.; Lovegrove, A.; Napier, J. A.; Shewry, P. R.; Beale, M. H. A metabolomic study of substantial equivalence of field-grown genetically modified wheat. *Plant Biotechnol. J.* **2006**, *4* (4), 381–392.

(14) Le Gall, G.; Colquhoun, I. J.; Davis, A. L.; Collins, G. J.; Verhoeven, M. E. Metabolite profiling of tomato (*Lycopersicon esculentum*) using <sup>1</sup>H NMR spectroscopy as a tool to detect potential unintended effects following a genetic modification. *J. Agric. Food Chem.* **2003**, *51* (9), 2447–2456.

(15) Coutinho, I. D.; Henning, L. M. M.; Döpp, S. A.; Nepomuceno, A.; Moraes, L. A. C.; Marcolino-Gomes, J.; et al. Flooded soybean metabolomic analysis reveals important primary and secondary metabolites involved in the hypoxia stress response and tolerance. *Environ. Exp. Bot.* **2018**, *153*, 176–187.

(16) Coutinho, I. D.; Henning, L. M. M.; Döpp, S. A.; Nepomuceno, A.; Moraes, L. A. C.; Marcolino-Gomes, J.; et al. Identification of primary and secondary metabolites and transcriptome profile of soybean tissues during different stages of hypoxia. *Data Brief* **2018**, *21*, 1089–1100.

(17) Spricigo, P. C.; Correia, B. S. B.; Borba, K. R.; Taver, I. B.; Machado, G. de O.; Wilhelms, R. Z.; et al. Classical food quality attributes and the metabolic profile of cambuci, a native brazilian atlantic rainforest fruit. *Molecules* **2021**, *26* (12), 3613.

(18) Ocampos, F. M. M.; de Souza, A. J. B.; Antar, G. M.; Wouters, F. C.; Colnago, L. A. Phytotoxicity of *Schiekia timida* Seed Extracts, a Mixture of Phenylphenalenones. *Molecules* **2021**, *26* (14), No. 4197, DOI: 10.3390/molecules26144197.

(19) de Souza, A. J. B.; Ocampos, F. M. M.; Catoia Pulgrossi, R.; Dokkedal, A. L.; Colnago, L. A.; Cechin, I.; Saldanha, L. L. NMR-Based Metabolomics Reveals Effects of Water Stress in the Primary and Specialized Metabolisms of *Bauhinia unguolata* L. (Fabaceae). *Metabolites* **2023**, *13* (3), 381.

(20) Ates, A. M.; Bukowski, M. Oil Crops Outlook: January 2023. USDA: Economic Research Service, OCS-23a, January 2023.

(21) Chen, K.-I.; Erh, M.-H.; Su, N.-W.; Liu, W.-H.; Chou, C.-C.; Cheng, K.-C. Soyfoods and soybean products: from traditional use to modern applications. *Appl. Microbiol. Biotechnol.* **2012**, *96* (1), 9–22.

(22) USDA. Brazil: Oilseeds and Products Update. Data and Analysis 2023 <https://www.fas.usda.gov/data/brazil-oilseeds-and-products-update-32>.

(23) da Silva, E. H. F. M.; Silva Antolin, L. A.; Zanon, A. J.; Soares Andrade, A.; de Souza, H. A.; dos Santos Carvalho, K.; et al. Impact assessment of soybean yield and water productivity in Brazil due to climate change. *Eur. J. Agron.* **2021**, *129*, No. 126329.

(24) Heino, M.; Puma, M. J.; Ward, P. J.; Gerten, D.; Heck, V.; Siebert, S.; Kummu, M. Two-thirds of global cropland area impacted by climate oscillations. *Nat. Commun.* **2018**, *9* (1), No. 1257, DOI: 10.1038/s41467-017-02071-5.

(25) Kulundžić, A. M.; Josipović, A.; Kočar, M. M.; Vuletić, M. V.; Dunić, J. A.; Varga, I. V.; Cesar, V.; Sudarić, A.; Lepedus, H. Physiological insights on soybean response to drought. *Agric. Water Manage.* **2022**, *268*, No. 107620.

(26) Yang, H.; Zhao, L.; Zhao, S.; Wang, J.; Shi, H. Biochemical and transcriptomic analyses of drought stress responses of LY1306 tobacco strain. *Sci. Rep.* **2017**, *7* (1), No. 17442.

(27) Dar, N. A.; Amin, I.; Wani, W.; Wani, S. A.; Shikari, A. B.; Wani, S. H.; Masoodi, K. Z. Abscisic acid: A key regulator of abiotic stress tolerance in plants. *Plant Gene* **2017**, *11*, 106–111.

(28) Kidokoro, S.; Watanabe, K.; Ohori, T.; Moriwaki, T.; Maruyama, K.; Mizoi, J.; et al. Soybean DREB1/CBF-type transcription factors function in heat and drought as well as cold stress-responsive gene expression. *Plant J.* **2015**, *81* (3), 505–518.

(29) Paul, M. J.; Nuccio, M. L.; Basu, S. S. Are GM Crops for Yield and Resilience Possible? *Trends Plant Sci.* **2018**, *23* (1), 10–16.

(30) Smyth, S. J.; Kerr, W. A.; Phillips, P. W. B. Global economic, environmental and health benefits from GM crop adoption. *Global Food Secur.* **2015**, *7*, 24–29.

(31) Zhao, L.; Hu, Y.; Chong, K.; Wang, T. ARAG1, an ABA-responsive DREB gene, plays a role in seed germination and drought tolerance of rice. *Ann. Bot.* **2010**, *105* (3), 401–409.

(32) Marinho, J. P.; Kanamori, N.; Ferreira, L. C.; Fuganti-Pagliarini, R.; Corrêa Carvalho, J.; de, F.; Freitas, R. A.; et al. Characterization of Molecular and Physiological Responses Under Water Deficit of Genetically Modified Soybean Plants Overexpressing the AtAREB1 Transcription Factor. *Plant Mol. Biol. Rep.* **2016**, *34* (2), 410–426.

(33) Barbosa, E. G. G.; Leite, J. P.; Marin, S. R. R.; Marinho, J. P.; de Fátima Corrêa Carvalho, J.; Fuganti-Pagliarini, R.; et al. Overexpression of the ABA-Dependent AREB1 Transcription Factor from *Arabidopsis thaliana* Improves Soybean Tolerance to Water Deficit. *Plant Mol. Biol. Rep.* **2013**, *31* (3), 719–730.

(34) Kavi Kishor, P. B.; Tiozon, R. N.; Fernie, A. R.; Sreenivasulu, N. Abscisic acid and its role in the modulation of plant growth, development, and yield stability. *Trends Plant Sci.* **2022**, *27* (12), 1283–1295.

(35) Parwez, R.; Aftab, T.; Gill, S. S.; Naeem, M. Abscisic acid signaling and crosstalk with phytohormones in regulation of environmental stress responses. *Environ. Exp. Bot.* **2022**, *199*, No. 104885.

(36) Umezawa, T.; Nakashima, K.; Miyakawa, T.; Kuromori, T.; Tanokura, M.; Shinozaki, K.; Yamaguchi-Shinozaki, K. Molecular basis of the core regulatory network in ABA responses: sensing, signaling and transport. *Plant Cell Physiol.* **2010**, *51* (11), 1821–1839.

(37) Fujita, Y.; Fujita, M.; Satoh, R.; Maruyama, K.; Parvez, M. M.; Seki, M.; et al. AREB1 Is a Transcription Activator of Novel ABRE-Dependent ABA Signaling That Enhances Drought Stress Tolerance in *Arabidopsis*. *Plant Cell* **2005**, *17* (12), 3470–3488.

(38) Yamaguchi-Shinozaki, K.; Shinozaki, K. Organization of cis-acting regulatory elements in osmotic- and cold-stress-responsive promoters. *Trends Plant Sci.* **2005**, *10* (2), 88–94.

(39) Zeng, H.; Wu, H.; Wang, G.; Dai, S.; Zhu, Q.; Chen, H.; et al. *Arabidopsis* CAMTA3/SR1 is involved in drought stress tolerance and ABA signaling. *Plant Sci.* **2022**, *319*, No. 111250.

(40) Fuganti-Pagliarini, R.; Ferreira, L. C.; Rodrigues, F. A.; Molinari, H. B. C.; Marin, S. R. R.; Molinari, M. D. C.; et al. Characterization of Soybean Genetically Modified for Drought

Tolerance in Field Conditions. *Front. Plant Sci.* **2017**, *8*, No. 448, DOI: 10.3389/fpls.2017.00448.

(41) Leite, J. P.; Barbosa, E. G. G.; Marin, S. R. R.; Marinho, J. P.; Carvalho, J. F. C.; Pagliarini, R. F.; et al. Overexpression of the activated form of the AtAREB1 gene (AtAREB1 $\Delta$ QT) improves soybean responses to water deficit. *Genet. Mol. Res.* **2014**, *13* (3), 6272–6286.

(42) Fuhrmann-Aoyagi, M. B.; de Fátima Ruas, C.; Barbosa, E. G. G.; Braga, P.; Moraes, L. A. C.; de Oliveira, A. C. B.; et al. Constitutive expression of Arabidopsis bZIP transcription factor AREB1 activates cross-signaling responses in soybean under drought and flooding stresses. *J. Plant Physiol.* **2021**, 257, No. 153338.

(43) Fehr, W. R.; Caviness, C. E. *Stages of Soybean Development* Iowa State University: Ames, IA; 1977.

(44) Flexas, J.; Bota, J.; Loreto, F.; Cornic, G.; Sharkey, T. D. Diffusive and metabolic limitations to photosynthesis under drought and salinity in C3 plants. *Plant Biol.* **2004**, *6* (3), 269–279.

(45) Coutinho, I. D.; Baker, J. M.; Ward, J. L.; Beale, M. H.; Creste, S.; Cavalheiro, A. J. Metabolite Profiling of Sugarcane Genotypes and Identification of Flavonoid Glycosides and Phenolic Acids. *J. Agric. Food Chem.* **2016**, *64* (21), 4198–4206.

(46) Cardozo, F. A.; Facchinatto, W. M.; Colnago, L. A.; Campana-Filho, S. P.; Pessoa, A. Bioproduction of N-acetyl-glucosamine from colloidal  $\alpha$ -chitin using an enzyme cocktail produced by *Aeromonas caviae* CHZ306. *World J. Microbiol. Biotechnol.* **2019**, *35* (8), 1141–1–1141-13.

(47) Johnson, R. L.; Schmidt-Rohr, K. Quantitative solid-state  $^{13}\text{C}$  NMR with signal enhancement by multiple cross polarization. *J. Magn. Reson.* **2014**, *239*, 44–49.

(48) Xia, J.; Wishart, D. S. Using MetaboAnalyst 3.0 for Comprehensive Metabolomics Data Analysis. *Curr. Protoc. Bioinf.* **2016**, *55*, 14.10.1–14.10.91.

(49) Ferreira, D. F. SISVAR: a computer statistical analysis system. *Sci. Agrotechnol.* **2011**, *35* (6), 1039.

(50) Coutinho, I. D.; Moraes, T. B.; Mertz-Henning, L. M.; Nepomuceno, A. L.; Giordani, W.; Marcolino-Gomes, J.; et al. Integrating High-Resolution and Solid-State Magic Angle Spinning NMR Spectroscopy and a Transcriptomic Analysis of Soybean Tissues in Response to Water Deficiency. *Phytochem. Anal.* **2017**, *28* (6), 529–540.

(51) Kempa, S.; Krasensky, J.; Dal Santo, S.; Kopka, J.; Jonak, C. A Central Role of Abscisic Acid in Stress-Regulated Carbohydrate Metabolism. *PLoS One* **2008**, *3* (12), No. e3935, DOI: 10.1371/journal.pone.0003935.

(52) Thalmann, M.; Santelia, D. Starch as a determinant of plant fitness under abiotic stress. *New Phytol.* **2017**, *214* (3), 943–951.

(53) Carvalho, A. M.; Bustamante, M. M. C.; Alcântara, F. A.; Resck, I. S.; Lemos, S. S. Characterization by solid-state CPMAS  $^{13}\text{C}$  NMR spectroscopy of decomposing plant residues in conventional and no-tillage systems in Central Brazil. *Soil Tillage Res.* **2009**, *102* (1), 144–150.

(54) García, M. P.; Zhang, Y. B.; Hayes, J. A.; Salazar, A.; Zabortina, O. A.; Hong, M. Structure and interactions of plant cell-wall polysaccharides by two- and three-dimensional magic-angle-spinning solid-state NMR. *Biochemistry* **2011**, *50* (6), 989–1000.

(55) Hatcher, P. G. Chemical structural studies of natural lignin by dipolar dephasing solid-state  $^{13}\text{C}$  nuclear magnetic resonance. *Org. Geochem.* **1987**, *11* (1), 31–39.

(56) Iulianelli, G. C. V.; Tavares, M. I. B. Application of solid-state NMR spectroscopy to evaluate cassava genotypes. *J. Food Compos. Anal.* **2016**, *48*, 88–94.

(57) Lemma, B.; Nilsson, I.; Kleja, D. B.; Olsson, M.; Knicker, H. Decomposition and substrate quality of leaf litters and fine roots from three exotic plantations and a native forest in the southwestern highlands of Ethiopia. *Soil Biol. Biochem.* **2007**, *39* (9), 2317–2328.

(58) Mutungi, C.; Passauer, L.; Onyango, C.; Jaros, D.; Rohm, H. Debranched cassava starch crystallinity determination by Raman spectroscopy: Correlation of features in Raman spectra with X-ray

diffraction and  $^{13}\text{C}$  CP/MAS NMR spectroscopy. *Carbohydr. Polym.* **2012**, *87* (1), 598–606.

(59) Knicker, H.; Lüdemann, H.-D. N-15 and C-13 CPMAS and solution NMR studies of N-15 enriched plant material during 600 days of microbial degradation. *Org. Geochem.* **1995**, *23* (4), 329–341.

(60) Forato, L. A.; Colnago, L. A.; Garrat, R. C.; Lopes, M. A. Identification of free fatty acids in maize protein bodies and purified alpha zeins by  $(^{13}\text{C}$  and  $^1\text{H})$  nuclear magnetic resonance. *Biochim. Biophys. Acta* **2020**, *1543* (1), 106–114.

(61) Rodziewicz, P.; Swarczewicz, B.; Chmielewska, K.; Wojakowska, A.; Stobiecki, M. Influence of abiotic stresses on plant proteome and metabolome changes. *Acta Physiol. Plant.* **2014**, *36* (1), 1–19.

(62) Zeeman, S. C.; Smith, S. M.; Smith, A. M. The breakdown of starch in leaves. *New Phytol.* **2004**, *163* (2), 247–261.

(63) Santelia, D.; Lunn, J. E. Transitory Starch Metabolism in Guard Cells: Unique Features for a Unique Function. *Plant Physiol.* **2017**, *174* (2), 539–549.

(64) Du, Y.; Zhao, Q.; Chen, L.; Yao, X.; Zhang, H.; Wu, J.; Xie, F. Effect of Drought Stress during Soybean R2-R6 Growth Stages on Sucrose Metabolism in Leaf and Seed. *Int. J. Mol. Sci.* **2020**, *21* (2), No. 618, DOI: 10.3390/ijms21020618.

(65) Boyer, J. S. Drought decision-making. *J. Exp. Bot.* **2010**, *61*, 3493 DOI: 10.1093/jxb/erq231.

(66) Zanella, M.; Borghi, G. L.; Pirone, C.; Thalmann, M.; Pazmino, D.; Costa, A.; et al.  $\beta$ -amylase 1 (BAM1) degrades transitory starch to sustain proline biosynthesis during drought stress. *J. Exp. Bot.* **2016**, *67* (6), 1819–1826.

(67) Tang, Y.; Sun, X.; Wen, T.; Liu, M.; Yang, M.; Chen, X. Implications of terminal oxidase function in regulation of salicylic acid on soybean seedling photosynthetic performance under water stress. *Plant Physiol. Biochem.* **2017**, *112*, 19–28.

(68) Ohashi, Y.; Nakayama, N.; Saneoka, H.; Fujita, K. Effects of drought stress on photosynthetic gas exchange, chlorophyll fluorescence and stem diameter of soybean plants. *Biol. Plant.* **2006**, *50* (1), 138–141.

(69) Singh, R.; Parihar, P.; Singh, S.; Mishra, R. K.; Singh, V. P.; Prasad, S. M. Reactive oxygen species signaling and stomatal movement: Current updates and future perspectives. *Redox Biol.* **2017**, *11*, 213–218.

(70) Ohlrogge, J.; Browse, J. Lipid biosynthesis. *Plant Cell* **1995**, *7* (7), 957–970.